NASA TM X-176

NASA TM X-176

TECHNICAL MEMORANDUM
X-176

EXPERIMENTAL AND CALCULATED SUPERSONIC FLUTTER CHARACTERISTICS OF MODELS OF THE X-15 HORIZONTAL AND VERTICAL TAILS

By William T. Lauten, Jr., and Robert W. Hess

Langley Research Center
Langley Field, Va.

NATIONAL AERONAUTICS AND SPACE ADMINISTRATION
WASHINGTON
December 1959

NATIONAL AERONAUTICS AND SPACE ADMINISTRATION

TECHNICAL MEMORANDUM X-176

EXPERIMENTAL AND CALCULATED SUPERSONIC FLUTTER CHARACTERISTICS OF MODELS OF THE X-15 HORIZONTAL AND VERTICAL TAILS*

By William T. Lauten, Jr., and Robert W. Hess

SUMMARY

A series of tests have been conducted at Mach numbers of 1.64, 2.0, 3.0, and 4.0 to investigate the possibility of flutter on dynamically and elastically scaled models of the all-movable horizontal- and vertical-tail surfaces of the X-15 airplane. No flutter was obtained on the scaled models.

Flutter was obtained on four weakened models of the horizontal tail at Mach numbers of 1.64, 2.0, and 3.0 and one weakened vertical-tail model at a Mach number of 3.0. The test results and structural information are presented. Also presented are the results of flutter calculations using aerodynamic forces derived from piston theory. The agreement between calculated and experimental flutter speeds is very good at a Mach number of 3.0 for the horizontal tail, but at the lower Mach numbers the agreement is less satisfactory.

INTRODUCTION

Flutter characteristics of various components of the X-15 airplane have been determined at the Langley Research Center. As part of this program, tests have been made on dynamically and elastically scaled models of the X-15 components in the various speed ranges of the airplane. Previous tests on the X-15 components for hypersonic speeds are reported in references 1 and 2.

*Title, Unclassified.

This paper presents the results of tests in the Langley 9- by 18-inch supersonic aeroelasticity tunnel of models of the horizontal- and vertical-tail surfaces at Mach numbers of 1.3, 2.0, 3.0, and 3.98. Since none of the scale models fluttered, the results that are presented are for model surfaces whose stiffness has been reduced until flutter occurred. A comparison is made with calculations in which the aerodynamic forces are derived from piston theory. (See ref. 3.) The first three natural modes of the horizontal-tail models and the first two natural modes of the vertical-tail model were used in the calculation and were experimentally determined by the method outlined in reference 4.

SYMBOLS

a	speed of sound, ft/sec
b	root semichord of model, ft
c	local semichord, ft
f	frequency, cps
h	mode shape, $\frac{\text{Displacement of any point on surface}}{\text{Displacement of point of maximum displacement}}$
l	span of model, ft
M	Mach number
m	mass of model segments, slugs
Δm	mass of increments of model, slugs
μ	model to air mass density ratio, $\frac{\text{Mass of wing}}{\pi\rho\int_0^l c^2 dy}$
ω	frequency, radians/sec
q	dynamic pressure, $\frac{1}{2}\rho V^2$, lb/sq ft
ρ	air density, slugs/cu ft

V	velocity, fps
y	spanwise coordinate

Subscripts:

1,2,3,4	indicate natural modes in ascending order of frequency
e	experimental flutter data
c	calculated flutter data

MODEL DESCRIPTION

All models were supplied by the manufacturer. Although the models were of similar construction, they were scaled in stiffness and mass on the basis of the dynamic pressure available in the test facility. Since the available dynamic pressure decreases with an increase in Mach number above $M = 2$, the models designed for the higher Mach numbers were lighter and more flexible as the Mach number increased above $M = 2$.

The models are identified in the text by the following scheme: HT and VT designate horizontal- and vertical-tail, respectively. The suffix contains the model number and the letter H or C. The suffix C designates those models which represent the airplane in the cold condition, whereas the suffix H designates the models which have been weakened to represent the airplane in the hot condition. For example, a model designated VT-2 is vertical-tail model 2 whereas model HT-4H is horizontal-tail model 4 which has been weakened to represent the airplane in the hot condition.

Horizontal Tail

The models of the horizontal stabilizer were 1/12 scale with an exposed surface aspect ratio of approximately 2.5, a taper ratio of 0.305, and a sweep angle of 45° at the quarter-chord line. The airfoil section was an NACA 66A005 modified so that it was 1 percent thick at the trailing edge with a straight-line fairing to the point of tangency. The airfoil ordinates are listed in table I.

Of the five horizontal-tail models of this investigation, four were designed to simulate surfaces reduced in stiffness by aerodynamic heating. The stiffness of the fifth model was not reduced and represented the case of the airplane not weakened by aerodynamic heating. Since no flutter

was obtained on the dynamically scaled models, the spindle spring restraint was reduced below the scaled values until flutter occurred.

All the horizontal-tail models were built with an aluminum box spar and rib construction. Small lead weights were distributed over the plan form in order to obtain the proper dynamic characteristics. To obtain the airfoil shape the section was filled with balsa and covered with lightweight silk. Figure 1 is an X-ray picture which shows typical construction.

A top-view drawing of the model mounted in the test section is shown in figure 2(a). The model base block served as a model mount and also as a spacer to support the model in the airstream beyond the tunnel boundary layer. A reflection plane, also shown in figure 2(a), was attached to the model base block just inboard of the wing root. The model was supported in its base block by means of two flexure pivot springs which simulated the spindle bearings of the prototype. The pivot was at 25 percent of the mean aerodynamic chord. A spring was mounted ahead of the model spindle and attached to the spindle with a screw as is shown in figure 2(b). The stiffness of the pitch spring and the pivot support combined to simulate the actuator stiffness of the prototype.

L
2
8
0

Vertical Tail

The vertical-tail models were 1/12 scale with an aspect ratio of 0.359 and a leading-edge sweep angle of 29°. The airfoil section was a wedge with an enclosed angle of 10°. Figure 3 shows top- and end-view drawings of the model as mounted in the test section. The vertical tail was built in two parts. Approximately one-fourth of the span was rigidly attached to the base block. On one model speed brakes comprised some 34 percent of the rear portion of the inboard section. Figure 4 is a photograph of the trailing edge of this model showing the speed brakes extended. The movable portion of the tail was attached to a spar which was attached to both the fixed portion and the model base block with springs.

Two models of the vertical tail were tested; one constructed with a magnesium frame covered with sheet balsa and silk did not flutter. This model had the speed brakes and is shown in figure 4. The second model which did flutter was much lighter and weaker. An X-ray photograph of this model is shown in figure 5. The spar was formed by wrapping a balsa box with aluminum-alloy sheet. The tail was then attached to the supporting spindle at the root-spar cap which was integral with the model and may be seen as the dark area at the root of the movable portion of the vertical tail. The fixed portion of the second model was not equipped with speed brakes.

INSTRUMENTATION

A recording oscillograph was used to obtain a continuous record during each test of tunnel stagnation, temperature, and pressure. Signals from strain gages mounted on the model spar were recorded on the same record and were used to determine flutter onset and frequency. Motion pictures, at 1,000 frames per second, were taken of the model during each tunnel run.

LABORATORY MEASUREMENTS

Prior to each run the frequencies and node lines for the first four natural modes were determined for the horizontal tail and the first two modes for the vertical tail. Figures 6(a) and 6(b) show typical sets of node lines.

The mode shapes were determined by the method of reference 4 on at least one, usually the stiffest wing in each series of tests. These mode shapes are presented in tables II to VII.

Horizontal Tail

After flutter testing was completed, the horizontal-tail models which were damaged but not completely destroyed were cut up in order to determine the section properties. The pitch inertia, roll inertia (about the strip center of gravity), and mass of the strips shown in figure 7 are given in table VIII. The section mass moment of inertia was determined by use of a bifilar suspension. The mass distribution in each section was also determined. Since the small lead weights cause discontinuities in the chordwise mass distribution, the streamwise sections were cut into small blocks. The apparently random distribution of cuts shown in figure 7 was decided upon to minimize the amount of mass lost in cutting. Table IX lists the mass of the blocks shown in figure 7 but does not include the mass of material lost in cutting.

Although the model designated as HT-7C was destroyed during the testing, its construction was so nearly identical to that of model HT-1H that a mass distribution for HT-7C was generated by consideration of the differences in the location and mass of the lead weights in the two models and the total mass of the model determined before testing. This mass distribution is also given in table IX.

Vertical Tail

It was necessary to calculate the mass distribution of the vertical-tail model VT-2 since it was destroyed by flutter. The thickness of the aluminum-alloy-spar skin, 0.005 inch, and the weight of the lead ballast and spar attachment cap were known. (See fig. 5.) The balsa sheet was assumed to be 0.0625 inch thick with a density of 6 pounds per cubic foot. The total weight of the vertical-tail model as determined from the summation of the measured and calculated weights of the various parts was within 2 percent of the total measured weight of the model.

Chordwise mass distribution curves, based on the previously mentioned assumptions, are given in figure 8. The ordinates of these curves are in slugs per square foot of control surface area and are based on the thickness and density of material at a particular point. For 10-percent span to 90-percent span the values for that portion of the chord which includes the spar have been adjusted to include the mass of the spar webs. The mass of the trailing edge, the mass of the lead balance weights, and the mass of the spar cap are not included. Neither is the mass of the two intermediate ribs included. The masses of the balance weights and the spar caps are shown in figure 5. The mass of increments of the two intermediate ribs and the trailing edge is given in table X.

Since these discrete masses are difficult to represent on a mass distribution curve, they are added into the flutter calculations as an incremental correction after the generalized mass of the model is calculated by utilizing the mass distribution curves.

COMPARISON OF FREQUENCY SPECTRUM, MODE SHAPES, AND NODAL PATTERNS FOR MODELS AND PROTOTYPE

Information on the tail surfaces of the prototype has become available and is compared with the vibration characteristics of the models. The full-scale information was obtained in vibration surveys made preliminary to some tests of full-scale tail surfaces in the Langley 9- by 6-foot thermal structures tunnel.

A comparison of the nodal patterns and frequency spectrums of the models and prototype are shown in figure 6(a) for the horizontal tail and in figure 6(b) for the vertical tail. A graphical comparison of the second mode of models HT-7C and HT-8H with the second mode of the prototype is shown in figure 9. The prototype modes which were measured are presented in tabular form in table XI.

TEST RESULTS

A summary of the test results is listed in table XII. The table lists the tunnel conditions at flutter. For model HT-8H, where no flutter was obtained on the weakest feasible configuration, maximum q is listed. Also listed are the density ratio of model mass to air mass μ, the model natural frequencies, the flutter frequency, and the stiffness-altitude parameter $\frac{b\omega_2}{a}\sqrt{\mu}$, where ω_2 is the frequency of the second natural mode in radians per second. The results of the flutter tests are also presented graphically in figures 10(a) and 10(b) which are plots of the stiffness-altitude parameter against Mach number for the horizontal and vertical tails, respectively. In these figures a constant dynamic pressure is a straight line through the origin. The flutter region is below and to the right of the flutter boundary, larger values of the stiffness-altitude parameter indicating less likelihood of flutter. Also shown is an airplane flight line based on a constant dynamic pressure of 2,500 pounds per square foot.

Horizontal Tail

No flutter was obtained on any of the dynamically scaled models of the horizontal tail at the Mach number for which they are designed. In order to obtain flutter information, the spring restraint was reduced below scaled values until flutter occurred. A comparison of the airplane flight path and the experimental results, plotted in figure 10(a), indicates that the flutter margin established by the models is smallest at M = 1.64. Since the stiffness-altitude parameter is inversely proportional to the square root of the dynamic pressure, it can be noted that at this Mach number the dynamic pressure corresponding to the experimental flutter point is 60 percent greater than the dynamic pressure corresponding to the flight path.

Vertical Tail

No flutter was obtained on the first vertical tail tested, model VT-1. The tests were partially inconclusive in that the speed brakes of the model were bottomed out on the stops by the aerodynamic loading before the desired dynamic pressure was obtained. This result was due to the fact that the spring stiffness of the speed brake was determined from frequency considerations and that the spring was not large enough to be preloaded to a point where it could withstand the aerodynamic loads. The tests were extended to the maximum available dynamic pressure with the weakest feasible root restraint in an effort to obtain flutter on the all-movable portion of the surface.

After no flutter was obtained on the first model, a second model VT-2 was constructed, as described in the section "Model Description," and tested at $M = 3$. This model fluttered to destruction; the results are presented graphically in figure 10(b). At a Mach number of 3 the experimental flutter point is at a $\frac{b\omega_2}{a}\sqrt{\mu}$ of 3.5 whereas the flight boundary is at a $\frac{b\omega_2}{a}\sqrt{\mu}$ of 9; thus, a very large margin of safety is indicated.

CALCULATED RESULTS

Modal-type flutter analyses were made by using the method of calculation set forth in reference 5. Aerodynamic forces were based on piston theory (ref. 3) which assumes that the local pressure on one point of the wing is a function only of the downwash velocity at that point and is independent of disturbances at other points of the wing. The first three natural modes of the horizontal tail and the first two natural modes of the vertical tail were used in the calculations, the mode shapes having been determined by the method of reference 4. The results of these calculations are summarized in table XI and are compared graphically with the experimental results in figures 10(a) and 10(b).

Horizontal Tail

The agreement between experimental and calculated flutter speeds for the horizontal tail at $M = 3.0$ was very good, with a difference of only 1 percent in the conservative direction. As might be expected when using piston theory, the agreement at the lower Mach numbers was not as good. The difference between the two values was 11 percent at $M = 2.0$ and 16 percent at $M = 1.64$, both unconservative. Although no flutter was obtained at $M = 3.98$, in view of the agreement between experimental and calculated values at $M = 3.0$, it was felt to be worthwhile to make similar calculations for the model tested at $M = 3.98$. These calculations showed that flutter should occur at a higher dynamic pressure than was available at this Mach number.

As a matter of interest, and as a check on the effects of possible inaccuracies in the determination of mode shape, the mode shape of the second mode of the horizontal-tail model, the mode to which these particular calculations are most sensitive, was arbitrarily changed by decreasing the deflection of the trailing edge by 20 percent and the deflection of the 75-percent chord line 10 percent. This change in mode shape is felt to be greater than any expected experimental inaccuracies. The resultant

calculated flutter speed at a Mach number of 3.0 was 3.4 percent lower than the original calculated value.

A second alternate calculation was made by using a less exact mass distribution. Instead of several mass increments along each streamwise strip, only three were used. These were the portion of the strip ahead of the spar, the spar section, and the portion of the strip behind the spar. The mode shapes used were the same as those for the original calculation. This modification resulted in a calculated speed which was 6.3 percent lower than the original value.

A third alternate calculation was made by omitting the third mode from the calculations. This variation in the input data resulted in a calculated speed which was 7.5 percent higher than the original value.

It is interesting to note that for this particular model the introduction of the first two variations (change in mode shape and mass distribution), which might occur as a result of experimental errors or approximation, result in a more conservative flutter speed. The omission of the higher frequency mode raises the calculated flutter speed and thus tends to be unconservative.

Vertical Tail

The results of the flutter calculations for model VT-2 are presented in table XII and figure 10(b). It may be seen that the calculated values are 28 percent conservative. There is no obvious reason why the difference between experimental and calculated results for the vertical tail is so much larger than the difference between the same two quantities for the horizontal tail. The lower aspect ratio and the unconventional airfoil shape of this configuration may be contributing factors.

CONCLUSIONS

Tests have been made on dynamically and elastically scaled models of the all-movable horizontal and vertical surfaces of the X-15 airplane to investigate the possibility of flutter. The models with design stiffness did not flutter. Flutter points were obtained at Mach numbers of 1.64, 2.0, and 3.0 on weakened models of the horizontal tail and at a Mach number of 3.0 on a weakened model of the vertical tail.

1. The minimum difference in dynamic pressure between the tentative flight path and the experimental model flutter boundary of the two surfaces occurs at a Mach number of 1.64. Based on the stiffness-altitude

parameter the flutter dynamic pressure is 60 percent greater than the expected dynamic pressure at this Mach number.

2. The agreement between calculated and experimental flutter speeds was excellent for the horizontal tail at a Mach number of 3, but the calculated values tended to deviate, and become unconservative, from the experimental values at Mach numbers of 2 and 1.64.

3. Flutter was only obtained on one model of the vertical tail at a Mach number of 3. This result indicated that the airplane vertical tail has a very large margin of safety from flutter at this Mach number. A comparison of the experimental with the calculated flutter speed showed that the calculated speed was 28 percent lower than the measured speed.

Langley Research Center,
National Aeronautics and Space Administration,
Langley Field, Va., August 19, 1959.

REFERENCES

1. Lauten, William T., Jr., Levey, Gilbert M., and Armstrong, William O.: Investigation of an All-Movable Control Surface at a Mach Number of 6.86 for Possible Flutter. NACA RM L58B27, 1958.

2. Gibson, Frederick W., and Mixson, John S.: Flutter Investigation at a Mach Number of 7.2 of Models of the Horizontal- and Vertical-Tail Surfaces of the X-15 Airplane. NASA MEMO 4-14-59L, 1959.

3. Ashley, Holt, and Zartarian, Garabed: Piston Theory - A New Aerodynamic Tool for the Aeroelastician. Jour. Aero. Sci., vol. 23, No. 12, Dec. 1956, pp. 1109-1118.

4. Hanson, Perry W., and Tuovila, W. J.: Experimentally Determined Natural Vibration Modes of Some Cantilever-Wing Flutter Models by Using an Acceleration Method. NACA TN 4010, 1957.

5. Morgan, Homer G., Huckel, Vera, and Runyan, Harry L.: Procedure for Calculating Flutter at High Supersonic Speed Including Camber Deflections, and Comparison With Experimental Results. NACA TN 4335, 1958.

TABLE I.- ORDINATES FOR NACA 66A005 (MODIFIED) AIRFOIL

[Ordinates in percent of chord]

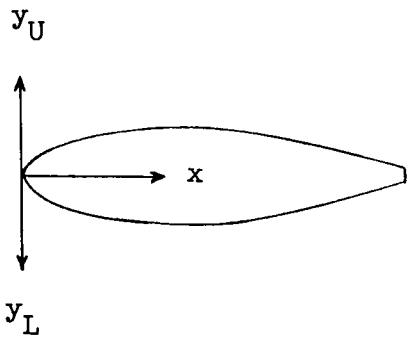

x	$y_U = y_L$
0	0
.10	.269
.25	.408
.50	.531
.75	.590
1.25	.650
2.50	.791
5.00	1.048
7.50	1.270
10.00	1.460
15.00	1.766
20.00	2.001
25.00	2.182
30.00	2.318
35.00	2.416
40.00	2.476
45.00	2.500
50.00	2.488
55.00	2.438
60.00	2.346
65.00	2.176
[a]67.00	2.085
100.00	.500

[a]Straight-line fairing from 67- to 100-percent chord.

TABLE II.- MODE SHAPE FOR MODEL HT-1H

Percent chord	Percent span										
	0	10	20	30	40	50	60	70	80	90	100
First mode											
0	-0.1504	-0.1200	-0.0800	-0.0384	0.0224	0.1072	0.2112	0.3296	0.4576	0.5920	0.7344
25	-.1008	-.0608	-.0160	.0384	.1056	.2000	.3024	.4160	.5376	.6624	.7920
50	-.0208	.0176	.0640	.1232	.2000	.2928	.3968	.5072	.6224	.7440	.8656
75	.0528	.0928	.1520	.2272	.3104	.4064	.5040	.6064	.7136	.8224	.9312
100	.1456	.1984	.2640	.3408	.4256	.5136	.6064	.7024	.8000	.9008	1.0000
Second mode											
0	1.000	0.995	0.982	0.957	0.935	0.922	0.912	0.903	0.899	0.892	0.889
25	.915	.914	.911	.906	.899	.888	.875	.865	.861	.859	.855
50	.799	.716	.644	.587	.546	.545	.586	.690	.770	.803	.806
75	-.775	-.826	-.850	-.855	-.851	-.838	-.814	-.733	-.203	.680	.733
100	-.945	-.940	-.932	-.925	-.915	-.901	-.884	-.858	-.655	-.115	.631
Third mode											
0	0.501	0.415	0.210	-0.484	-0.733	-0.819	-0.854	-0.855	-0.806	-0.637	0.142
25	.363	.127	-.274	-.564	-.672	-.718	-.728	-.709	-.628	.141	.552
50	.211	-.214	-.417	-.533	-.592	-.615	-.598	-.508	.252	.534	.664
75	-.233	-.335	-.409	-.449	-.449	-.399	-.155	.361	.625	.777	.860
100	-.450	-.382	-.274	-.121	.089	.343	.570	.727	.856	.948	1.000

TABLE III.- MODE SHAPE FOR MODEL HT-2H

Percent chord	Percent span										
	0	10	20	30	40	50	60	70	80	90	100
First mode											
0	-0.341	-0.272	-0.213	-0.122	-0.033	0.057	0.200	0.323	0.502	0.713	0.841
25	-.195	-.144	-.079	.009	.090	.177	.317	.454	.604	.777	.866
50	-.043	.012	.056	.122	.218	.306	.440	.591	.726	.857	.915
75	.084	.135	.191	.261	.370	.485	.616	.767	.850	.926	.957
100	.185	.259	.378	.502	.617	.744	.838	.915	.950	.978	1.000
Second mode											
0	0.993	1.000	0.967	0.903	0.888	0.890	0.916	0.931	0.921	0.883	0.834
25	.648	.703	.660	.586	.569	.559	.580	.607	.631	.676	.697
50	.228	.228	.187	.145	.116	.103	.130	.186	.282	.400	.566
75	-.166	-.248	-.328	-.386	-.429	-.441	-.390	-.276	-.062	.221	.428
100	-.676	-.738	-.800	-.841	-.852	-.841	-.741	-.552	-.230	.110	.359
Third mode											
0	0.501	0.415	0.210	-0.484	-0.733	-0.819	-0.854	-0.855	-0.806	-0.637	0.142
25	.363	.127	-.274	-.564	-.672	-.718	-.728	-.709	-.628	.141	.552
50	.211	-.214	-.417	-.533	-.592	-.615	-.598	-.508	.252	.534	.664
75	-.233	-.335	-.409	-.449	-.449	-.399	-.155	.361	.625	.777	.860
100	-.450	-.382	-.274	-.121	.089	.343	.570	.727	.856	.948	1.000

TABLE IV.- MODE SHAPE FOR MODEL HT-4H

Percent chord	Percent span										
	0	10	20	30	40	50	60	70	80	90	100
First mode											
0	-0.162	-0.140	-0.123	-0.094	-0.041	0.053	0.144	0.220	0.295	0.383	0.500
25	-.128	-.118	-.085	-.012	.080	.144	.203	.273	.355	.469	.628
50	-.064	-.007	.070	.120	.159	.199	.253	.326	.432	.568	.730
75	.097	.120	.147	.179	.217	.263	.321	.406	.537	.708	.913
100	.156	.184	.218	.258	.300	.352	.418	.513	.641	.806	1.000
Second mode											
0	0.894	0.799	0.702	0.604	0.506	0.436	0.417	0.474	0.625	0.847	1.000
25	.645	.518	.404	.308	.240	.207	.213	.303	.533	.708	.812
50	.294	.131	.006	-.067	-.082	-.036	.042	.151	.368	.593	.741
75	-.322	-.380	-.425	-.451	-.446	-.400	-.300	-.097	.173	.487	.693
100	-.650	-.722	-.766	-.771	-.713	-.607	-.474	-.319	-.083	.428	.692
Third mode											
0	0.501	0.415	0.210	-0.484	-0.733	-0.819	-0.854	-0.855	-0.806	-0.637	0.142
25	.363	.127	-.274	-.564	-.672	-.718	-.728	-.709	-.628	.141	.552
50	.211	-.214	-.417	-.533	-.592	-.615	-.598	-.508	.252	.534	.664
75	-.233	-.335	-.409	-.449	-.449	-.399	-.155	.361	.625	.777	.860
100	-.450	-.382	-.274	-.121	.089	.343	.570	.727	.856	.948	1.000

TABLE V.- MODE SHAPE FOR MODEL HT-7C

Percent chord	Percent span										
	0	10	20	30	40	50	60	70	80	90	100
First mode											
0	-0.218	-0.192	-0.158	-0.110	-0.047	0.036	0.137	0.252	0.385	0.525	0.675
25	-.148	-.106	-.058	.013	.060	.140	.237	.345	.468	.607	.752
50	-.027	.009	.044	.093	.155	.233	.326	.434	.557	.686	.825
75	.047	.095	.145	.200	.262	.336	.426	.527	.644	.765	.907
100	.188	.230	.271	.320	.376	.442	.525	.621	.735	.860	1.000
Second mode											
0	1.000	0.721	0.545	0.455	0.388	0.350	0.328	0.328	0.385	0.504	0.639
25	.549	.408	.307	.271	.259	.257	.255	.266	.336	.466	.598
50	.138	.131	.136	.149	.165	.182	.202	.234	.309	.436	.558
75	-.156	-.215	-.257	-.278	-.271	-.223	-.073	.175	.300	.415	.512
100	-.466	-.483	-.487	-.468	-.418	-.351	-.271	.058	.284	.400	.497
Third mode											
0	0.122	0.035	-0.053	-0.166	-0.335	-0.454	-0.505	-0.498	-0.375	-0.075	0.534
25	.026	-.044	-.122	-.221	-.316	-.368	-.371	-.317	-.171	.258	.659
50	-.084	-.132	-.179	-.236	-.284	-.298	-.274	-.195	.080	.474	.757
75	-.116	-.153	-.196	-.232	-.249	-.241	-.154	.118	.395	.629	.868
100	-.140	-.180	-.213	-.232	-.219	-.126	.124	.388	.600	.798	1.000

TABLE VI.- MODE SHAPE FOR MODEL HT-8H

Percent chord	Percent span										
	0	10	20	30	40	50	60	70	80	90	100
First mode											
0	-0.162	-0.148	-0.127	-0.090	-0.027	0.078	0.201	0.330	0.457	0.582	0.711
25	-.119	-.094	-.057	.008	.096	.188	.285	.402	.523	.645	.766
50	-.056	-.012	.047	.117	.201	.291	.393	.504	.613	.721	.832
75	.066	.107	.160	.227	.307	.395	.492	.596	.699	.807	.912
100	.152	.203	.262	.336	.418	.506	.600	.699	.799	.898	1.000
Second mode											
0	1.000	0.800	0.591	0.438	0.332	0.247	0.203	0.206	0.285	0.427	0.600
25	.418	.335	.256	.182	.129	.106	.106	.129	.200	.315	.459
50	.125	.042	-.024	-.070	-.094	-.099	-.059	.029	.141	.268	.409
75	-.191	-.214	-.265	-.271	-.274	-.259	-.168	-.097	.106	.235	.356
100	-.518	-.523	-.494	-.465	-.427	-.374	-.294	-.138	.062	.197	.291
Third mode											
0	-0.066	-0.067	-0.085	-0.141	-0.235	-0.392	-0.547	-0.656	-0.648	-0.473	-0.003
25	-.035	-.074	-.119	-.192	-.306	-.429	-.532	-.585	-.490	-.147	.344
50	-.028	-.085	-.153	-.231	-.316	-.394	-.406	-.335	-.113	.275	.591
75	.007	-.049	-.146	-.200	-.236	-.245	-.189	.028	.346	.645	.831
100	.006	-.077	-.092	-.116	-.095	.063	.272	.548	.739	.873	1.000

TABLE VII.- MODE SHAPES FOR MODEL VT-2

Percent chord	Percent span												
	0	10	20	30	35	40	50	60	65	70	80	90	100
First mode													
0	-0.329	-0.310	-0.293	-0.277	-0.273	-0.256	-0.238	-0.210	-0.198	-0.185	-0.156	-0.133	-0.126
25	-.116	-.069	-.039	-.001	.018	.024	.053	.093	.111	.116	.135	.153	.158
50	.310	.322	.337	.346	.350	.346	.354	.370	.375	.377	.380	.390	.396
75	.586	.602	.616	.630	.630	.641	.652	.662	.667	.670	.674	.691	.697
100	.820	.844	.873	.892	.901	.902	.919	.929	.932	.948	.965	.978	1.000
Second mode													
0	0.815	0.698	0.571	0.588	0.594	0.605	0.787	0.942	0.967	0.983	0.995	1.000	1.000
25	.501	.488	.486	.496	.500	.520	.549	.603	.685	.755	.843	.888	.913
50	-.075	.011	.218	.350	.383	.399	.421	.447	.462	.492	.539	.473	.490
75	-.014	-.546	-.490	-.467	-.456	-.438	-.314	-.063	.051	.123	.234	.440	.436
100	-.904	-.878	-.825	-.740	-.682	-.645	-.603	-.578	-.567	-.556	-.500	-.281	.407

TABLE VIII.- MASS PROPERTIES OF STREAMWISE STRIPS SHOWN IN FIGURE 7

Strip	Model HT-1H			Model HT-2H			Model HT-4H			Model HT-8H		
	Roll inertia, ft-lb-sec^2	Pitch inertia, ft-lb-sec^2	Mass, slugs	Roll inertia, ft-lb-sec^2	Pitch inertia, ft-lb-sec^2	Mass, slugs	Roll inertia, ft-lb-sec^2	Pitch inertia, ft-lb-sec^2	Mass, slugs	Roll inertia, ft-lb-sec^2	Pitch inertia, ft-lb-sec^2	Mass, slugs
I	5.701×10^{-7}	3.308×10^{-5}	1.9692×10^{-3}	7.545×10^{-7}	3.7917×10^{-5}	2.2412×10^{-3}	5.039×10^{-7}	2.0552×10^{-5}	1.2633×10^{-3}	23.050×10^{-7}	16.508×10^{-5}	8.1123×10^{-4}
II	1.644	.7967	.5881	2.182	.8067	.6050	1.141	.5525	.3428	2.799	.028	.1912
III	1.636	.7550	.5708	2.028	.8658	.5913	1.428	.8075	.5787	3.233	.232	.8958
IV	1.095	.5367	.4124	1.653	.5900	.5270	1.090	.3725	.3243	5.906	.499	1.1272
V	.761	.5219	.3894	1.458	.5300	.4807	.752	.2367	.2513	9.870	1.030	1.9137
VI	.769	.3879	.4101	1.200	.2875	.3844	.660	.1617	.2176	9.755	2.706	2.6643
VII	.619	.1329	.2295	1.067	.1899	.3565	.620	.1077	.2393	4.894	.744	1.1399
VIII	.641	.1448	.2799	.848	.0844	.2655	.439	.0330	.1435	14.591	1.262	1.8408
IX	.776	.0795	.2691	----------	----------	----------	----------	----------	----------	5.364	2.632	1.8842

TABLE IX.- MASS OF MODEL SEGMENTS SHOWN IN FIGURE 7

Chordwise increment	Streamwise strips												
	I	II	III	IV	V	VI	VII	VIII	IX	X	XI	XII	XIII
Model HT-1													
1	0.8260×10^{-4}	0.2832×10^{-4}	0.4874×10^{-4}	0.3766×10^{-4}	0.8521×10^{-4}	1.3358×10^{-4}	0.2875×10^{-4}	0.3819×10^{-4}	0.0687×10^{-4}	----------	----------	----------	----------
2	5.1363	.1949	.1684	.2817	.1649	.4984	.2692	.6676	.8831	----------	----------	----------	----------
3	2.1671	1.1931	1.2188	.8992	.9910	.4074	.3231	.3652	.4363	----------	----------	----------	----------
4	3.8424	2.7561	2.1628	1.3362	.8126	.6875	.6068	.5746	.8561	----------	----------	----------	----------
5	3.7839	.6606	.8440	.5843	.6004	.6149	.3786	.5340	.4086	----------	----------	----------	----------
6	2.6348	.2695	.1603	.5962	.4378	.4951	.1997	.2356	----------	----------	----------	----------	----------
7	.5586	.4615	.6094	----------	----------	----------	----------	----------	----------	----------	----------	----------	----------
8	.5636	----------	----------	----------	----------	----------	----------	----------	----------	----------	----------	----------	----------
Model HT-2													
1	1.2446×10^{-4}	0.3814×10^{-4}	0.5286×10^{-4}	0.2670×10^{-4}	0.5110×10^{-4}	0.4919×10^{-4}	0.6861×10^{-4}	0.9715×10^{-4}	----------	----------	----------	----------	----------
2	5.6288	.2761	.1242	1.2869	1.0192	1.2456	1.0530	.4519	----------	----------	----------	----------	----------
3	5.5182	.9499	.8807	1.0053	.6145	.4738	.9591	.7402	----------	----------	----------	----------	----------
4	3.0569	.4066	.2272	1.4958	1.1551	.7935	.5217	.4575	----------	----------	----------	----------	----------
5	2.9932	2.4909	.8052	.7785	.4747	.3799	.3305	----------	----------	----------	----------	----------	----------
6	.5414	.7498	.1715	.2157	.9990	.4276	----------	----------	----------	----------	----------	----------	----------
7	.5522	.3273	1.0863	.1831	----------	----------	----------	----------	----------	----------	----------	----------	----------
8	----------	.4146	----------	----------	----------	----------	----------	----------	----------	----------	----------	----------	----------
Model HT-4													
1	0.5740×10^{-4}	0.3460×10^{-4}	0.3037×10^{-4}	0.2070×10^{-4}	0.1894×10^{-4}	0.3952×10^{-4}	0.4213×10^{-4}	0.0390×10^{-4}	----------	----------	----------	----------	----------
2	1.7559	.3297	2.6537	.6078	.1060	.0815	.3863	.0601	----------	----------	----------	----------	----------
3	.8079	.2453	.2502	.3210	.0637	.0685	.4493	.1140	----------	----------	----------	----------	----------
4	.8093	1.7641	1.7834	1.4849	.1550	1.2246	.0283	.3167	----------	----------	----------	----------	----------
5	6.7187	.1636	.1797	.3177	1.3823	.0557	.8716	.1171	----------	----------	----------	----------	----------
6	.8320	.2936	.1906	.0842	.4254	.0880	.1034	.0843	----------	----------	----------	----------	----------
7	.4400	.2311	.3591	.1702	.1465	.2363	.0531	----------	----------	----------	----------	----------	----------
8	.5377	----------	----------	----------	----------	----------	.0513	----------	----------	----------	----------	----------	----------
Model HT-7													
1	0.9456×10^{-4}	2.2602×10^{-4}	0.5580×10^{-4}	0.4312×10^{-4}	0.2651×10^{-4}	0.3740×10^{-4}	0.7680×10^{-4}	0.1659×10^{-4}	0.0589×10^{-4}	----------	----------	----------	----------
2	2.3621	.2231	.1928	.3225	.1887	.5705	.0974	.3383	.2293	----------	----------	----------	----------
3	2.4809	1.3658	1.3953	1.0294	1.1345	.4664	.5988	.4181	.4994	----------	----------	----------	----------
4	4.3988	3.1551	2.4760	1.5297	.9303	.7870	.6947	.6578	.9801	----------	----------	----------	----------
5	4.3318	.7562	.9663	.6689	.6873	.7039	.4334	.6113	.4678	----------	----------	----------	----------
6	3.0163	.3085	.1836	.6888	.5062	.4665	.5146	.1316	----------	----------	----------	----------	----------
7	.6395	.4616	.2572	----------	----------	----------	----------	----------	----------	----------	----------	----------	----------
8	.5767	----------	----------	----------	----------	----------	----------	----------	----------	----------	----------	----------	----------
Model HT-8													
1	20.2349×10^{-5}	1.9116×10^{-5}	4.9932×10^{-5}	1.8518×10^{-5}	3.1405×10^{-5}	5.0486×10^{-5}	1.1208×10^{-5}	2.3538×10^{-5}	4.5249×10^{-5}	0.4135×10^{-5}	----------	----------	2.6311×10^{-5}
2	13.3733	----------	3.8512	2.7489	3.8478	3.6971	1.4494	2.7092	2.3949	.5347	0.3732×10^{-5}	----------	1.0860
3	30.9861	----------	----------	6.4850	9.7714	8.9375	5.6313	6.5542	5.3608	2.0814	2.0437	0.2657×10^{-5}	.9626
4	10.5594	----------	----------	----------	1.9403	4.7358	1.6041	3.3425	2.4964	.5854	1.5158	.2389	.9566
5	4.5009	----------	----------	----------	----------	3.7259	1.3159	2.9714	4.8905	.4861	2.2149	.4437	2.6455

TABLE X.- MASS INCREMENTS AT TRAILING EDGE AND RIBS FOR VT-2

(a) Trailing edge

	Percent span to center of gravity of increment									
	10	20	30	40	50	60	70	80	90	
Δm, slugs	3.330×10^{-6}	3.259×10^{-6}	3.189×10^{-6}	3.116×10^{-6}	3.045×10^{-6}	2.974×10^{-6}	2.902×10^{-6}	2.831×10^{-6}	2.759×10^{-6}	

(b) Rib 1

	Percent chord to center of gravity of increment									
	5	15	25	35	45	55	65	75	85	95
Δm, slugs	0.414×10^{-6}	1.242×10^{-6}	2.070×10^{-6}	2.897×10^{-6}	3.666×10^{-6}	4.553×10^{-6}	5.499×10^{-6}	6.209×10^{-6}	7.036×10^{-6}	7.923×10^{-6}

(c) Rib 2

	Percent chord to center of gravity of increment									
	5	15	25	35	45	55	65	75	85	95
Δm, slugs	0.359×10^{-6}	1.078×10^{-6}	(a)	2.508×10^{-6}	3.228×10^{-6}	3.943×10^{-6}	4.669×10^{-6}	5.379×10^{-6}	6.094×10^{-6}	6.815×10^{-6}

[a]Access hole.

TABLE XI.- MODE SHAPES FOR X-15 PROTOTYPE HORIZONTAL TAIL

Percent chord	Percent span										
	0	10	20	30	40	50	60	70	80	90	100
First mode											
0	-0.279	-0.183	-0.098	-0.018	0.086	0.171	0.256	0.345	0.458	0.586	0.737
25	-.176	-.098	-.014	.074	.162	.254	.350	.455	.578	.702	.834
50	-.056	.028	.119	.205	.295	.392	.486	.585	.688	.790	.895
75	.077	.186	.290	.385	.439	.562	.643	.722	.797	.871	.948
100	.218	.365	.488	.581	.664	.739	.801	.859	.902	.953	1.000
Second mode											
0	1.000	0.942	0.855	0.786	0.707	0.646	0.594	0.536	0.511	0.471	0.453
25	.560	.494	.420	.361	.320	.301	.294	.297	.299	.319	.346
50	.109	.080	.073	.054	.044	.044	.045	.078	.123	.173	.214
75	-.297	-.257	-.239	-.204	-.159	-.144	-.145	-.110	-.049	.029	.076
100	-.547	-.552	-.549	-.522	-.487	-.426	-.339	-.241	-.160	-.086	0
Third mode											
0	0.180	0.095	0.011	-0.080	-0.163	-0.228	-0.262	-0.187	-0.124	0.095	0.418
25	.107	.027	-.049	-.113	-.175	-.227	-.224	-.162	-.020	.212	.543
50	.019	-.639	-.127	-.169	-.202	-.218	-.175	-.083	.099	.307	.676
75	-.091	-.171	-.217	-.240	-.243	-.183	-.099	.052	.243	.502	.824
100	-.257	-.289	-.316	-.322	-.290	-.116	.042	.224	.460	.722	1.000

TABLE XII.- SUMMARY OF TEST RESULTS

Configuration	M	V_e, ft/sec	ρ, slugs/cu ft	$\left(\frac{b\omega_2}{a}\sqrt{\mu}\right)_e$	f_e, cps	μ	a, ft/sec	q, lb/sq ft	V_c, ft/sec	f_c, cps	f_1, cps	f_2, cps	f_3, cps	f_4, cps	$\left(\frac{b\omega_2}{a}\sqrt{\mu}\right)_c$
HT-1H	1.64	1,526	0.00243	4.57	247	49.45	930	2,840	1,826	268	136	330	515	650	3.79
HT-2H	2.0	1,734	.001925	5.10	279.5	66.4	867	2,890	1,959	238	128	296	485	640	4.59
HT-4H	3.0	2,171	.000872	5.85	185	89.7	724	2,050	2,144	199	96	244	415	550	5.91
HT-7C	1.64	1,505	.00331	4.75	267	37.0	918	3,738	1,704	314	162.5	391	725	1,000	4.20
HT-8H*	3.98	2,318	.000332	7.64	-----	148.5	582	890	2,900	148	63.4	200	318	433	6.18
VT-2	3.0	2,265	.00085	3.58	200	19.77	755	2,180	1,631	223	120	253	---	---	4.97

*No flutter.

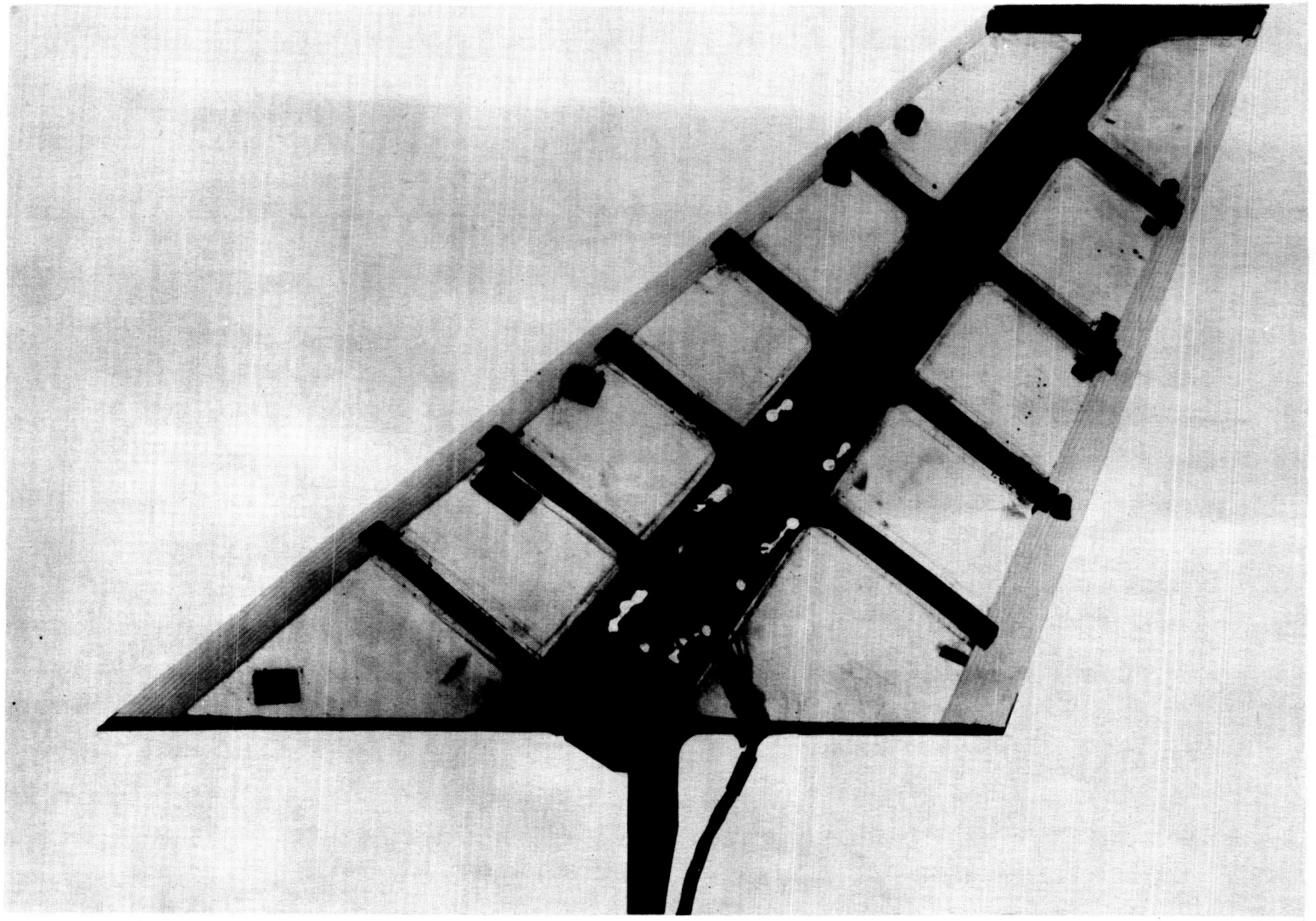

Figure 1.- X-ray photograph of model of horizontal tail showing typical construction. L-59-6023

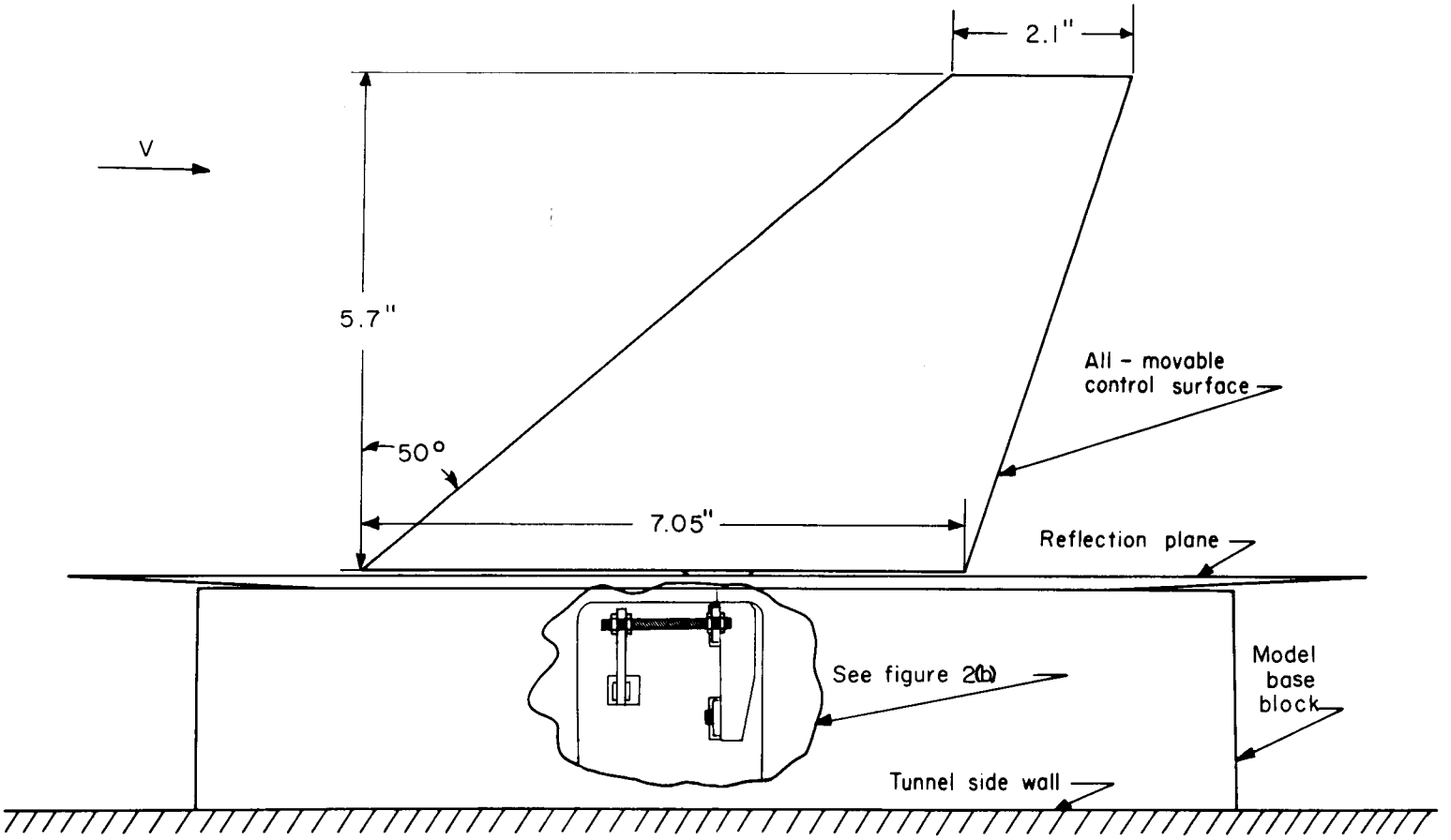

(a) Overall view.

Figure 2.- Model as mounted in tunnel.

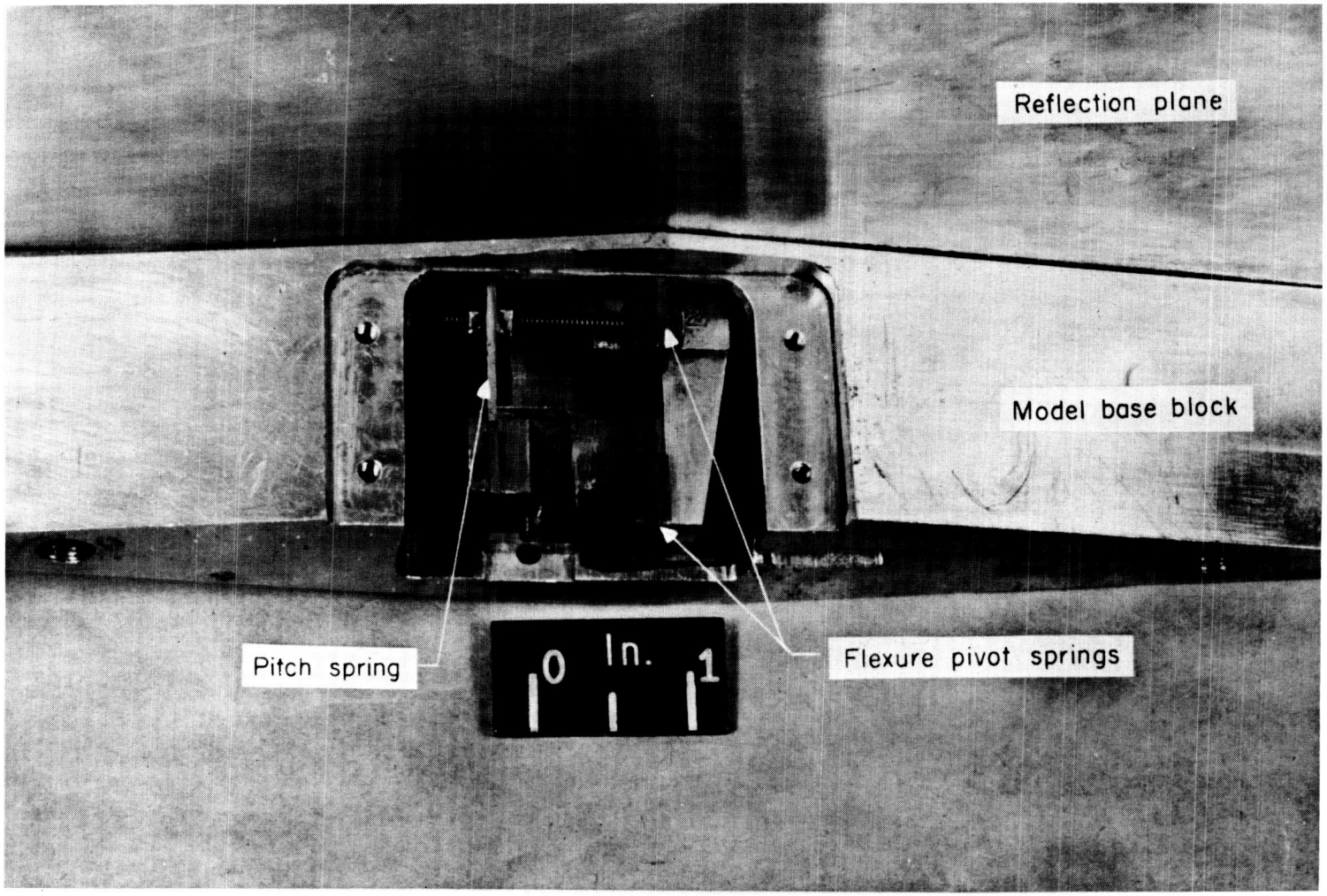

(b) Photograph showing detail of model restraint. L-57-4258.1

Figure 2.- Concluded.

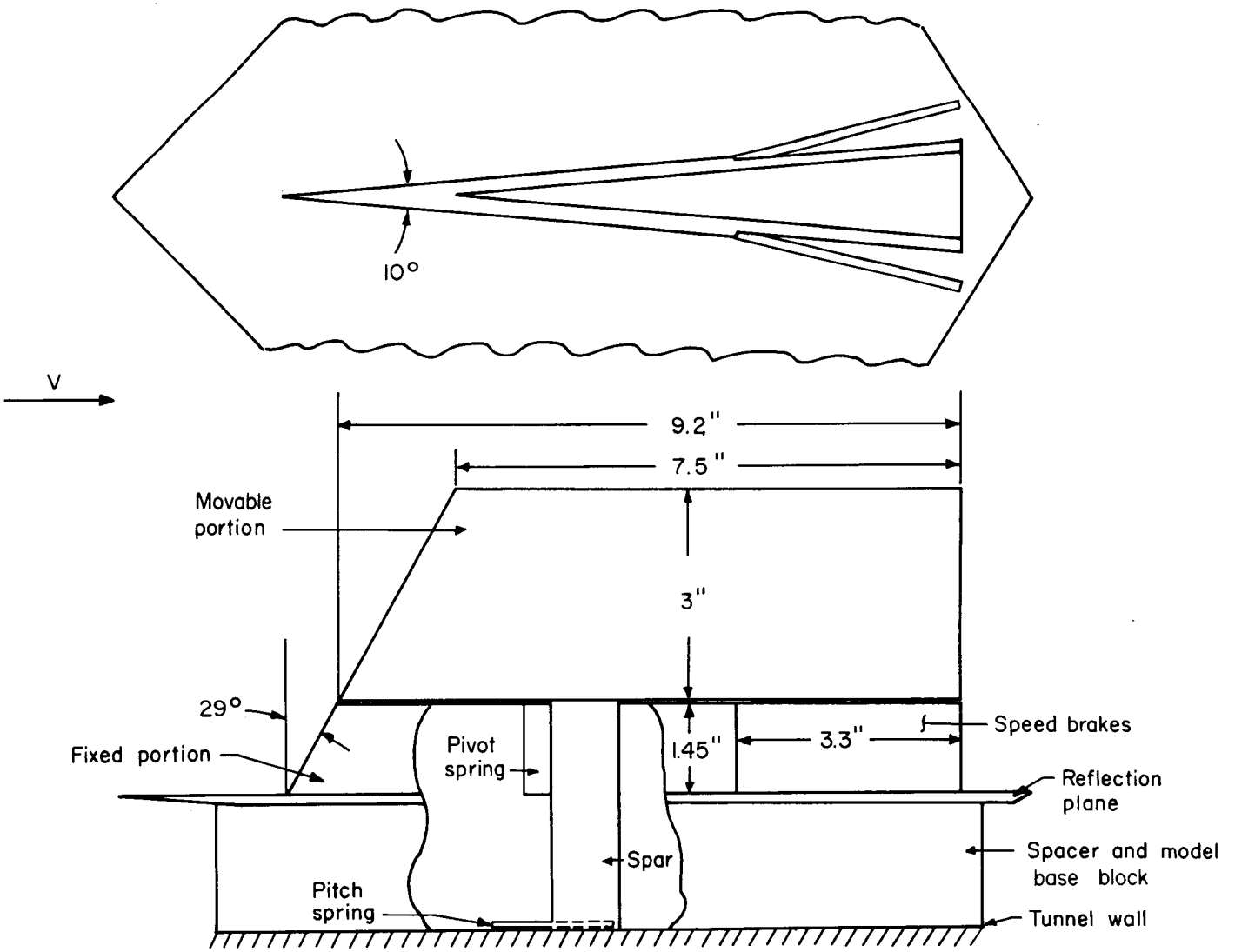

Figure 3.- Sketch of model of vertical tail.

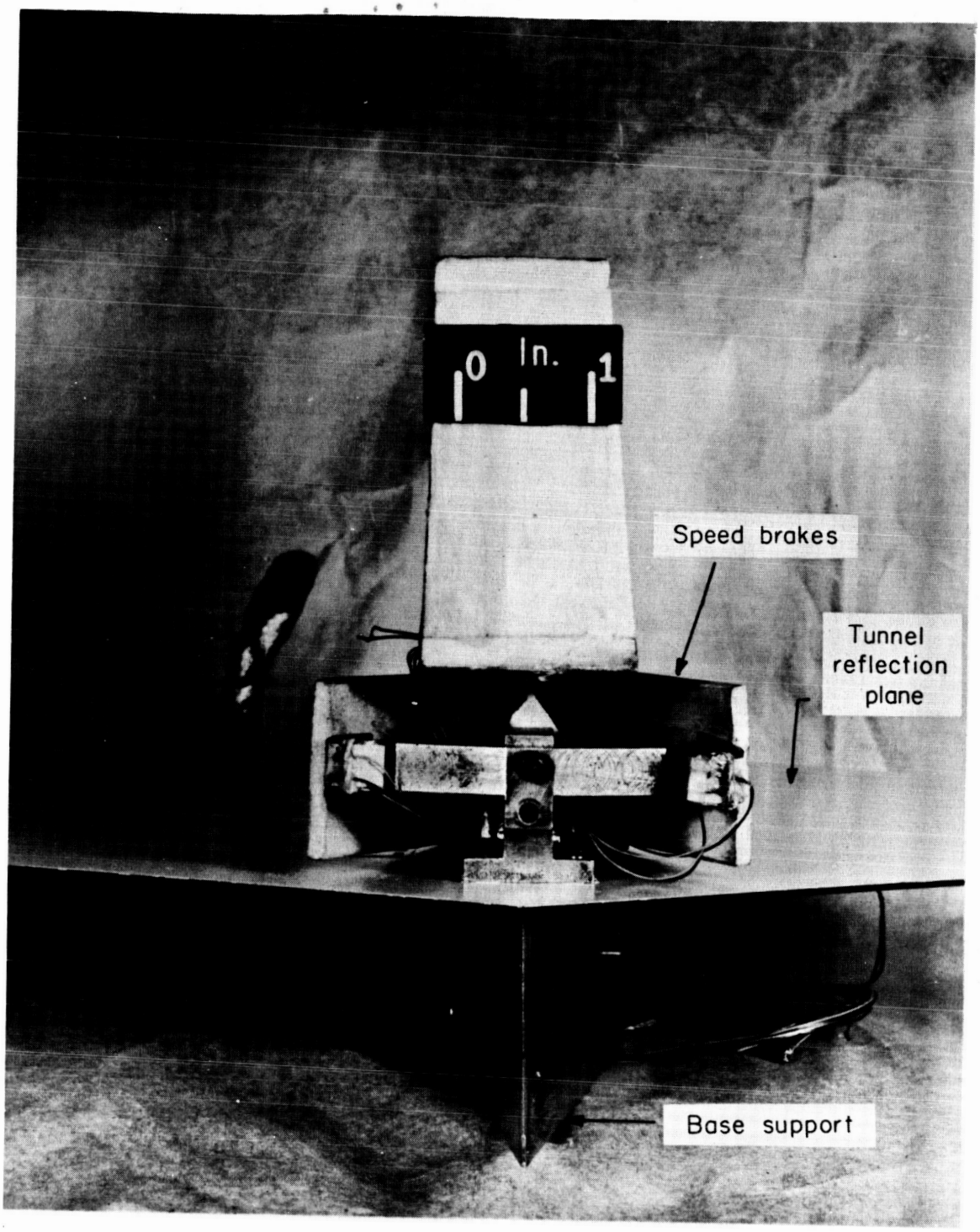

L-57-4260.1

Figure 4.- Photograph of trailing edge of model of vertical tail showing speed brakes extended.

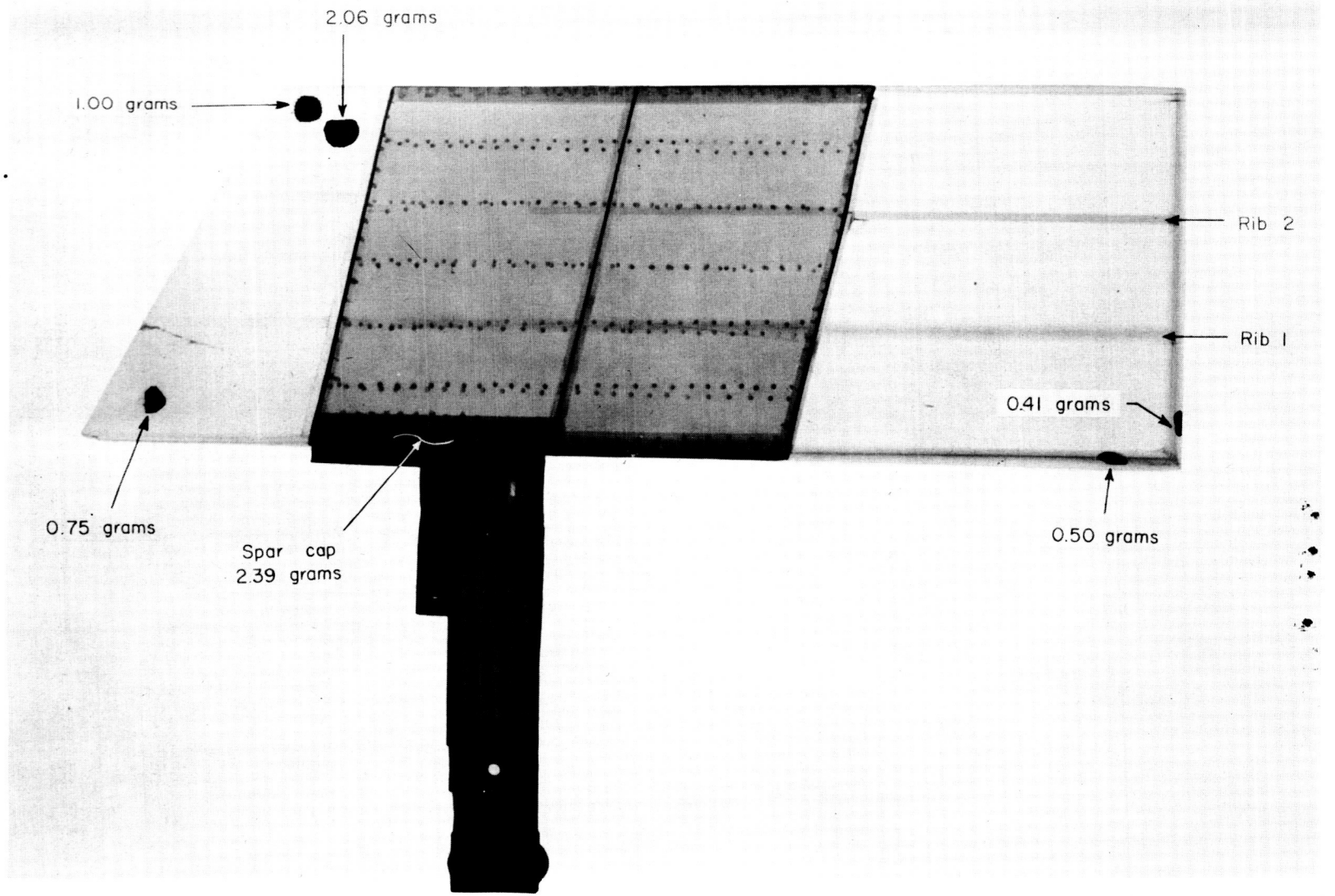

Figure 5.- X-ray photograph of model VT-2. L-59-6024

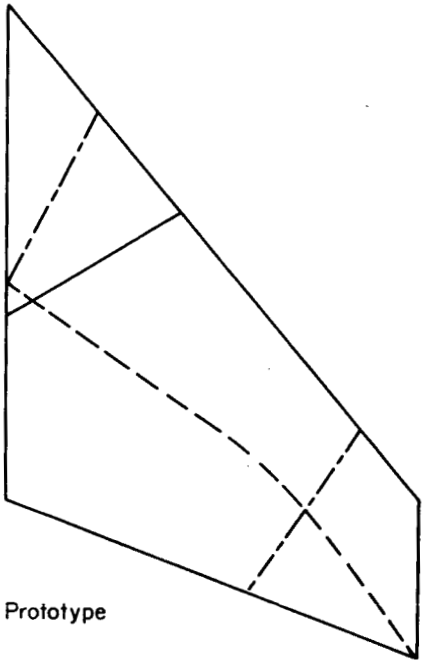

Prototype

Mode	Node line	Frequency
1 st	———	12.6 cps
2 nd	— — —	34.0 cps
3 rd	—·—	53.0 cps

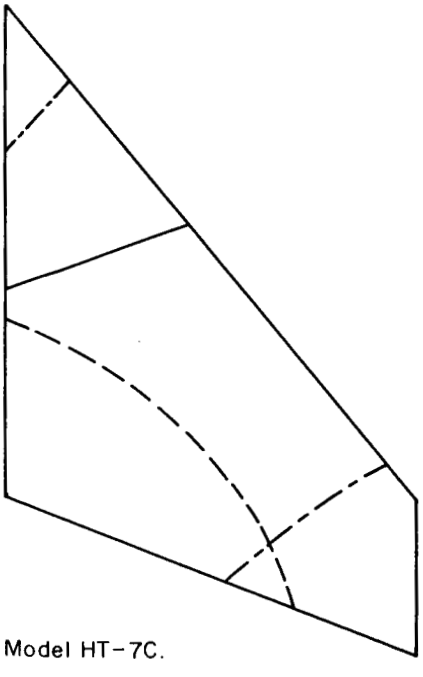

Model HT-7C.

Mode	Node line	Model frequency	Scaled prototype frequency
1 st	———	162.5 cps	151.2 cps
2nd	— — —	391.0 cps	408.0 cps
3 rd	—·—	725.0 cps	636.0 cps

(a) Horizontal tail.

Figure 6.- Comparison of nodal patterns and frequency spectrums of model and prototype tail surfaces.

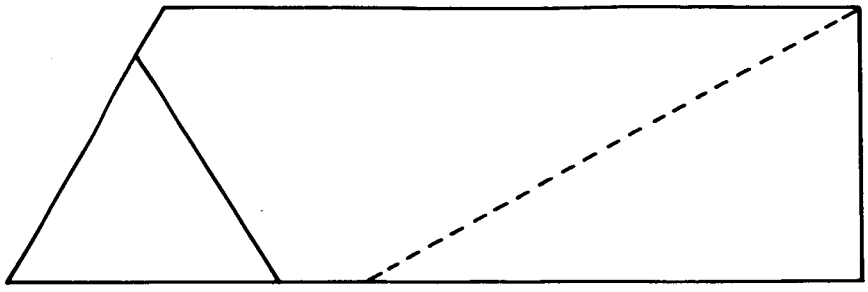

Prototype

Mode	Node line	Frequency
1 st	———	15 cps
2 nd	— — — —	34 cps

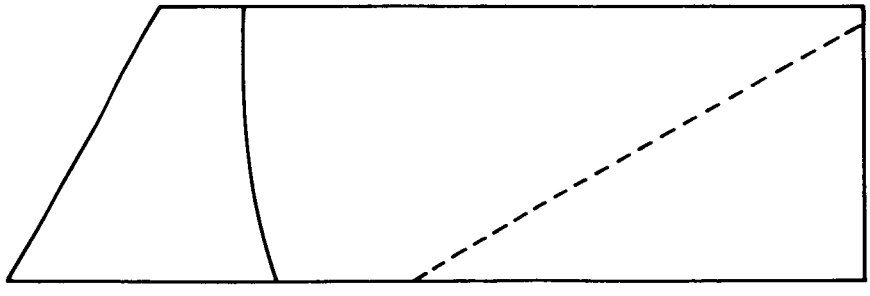

Model VT-2.

Mode	Node line	Frequency
1 st	———	120 cps
2 nd	- - - - -	253 cps

(b) Vertical tail.

Figure 6.- Concluded.

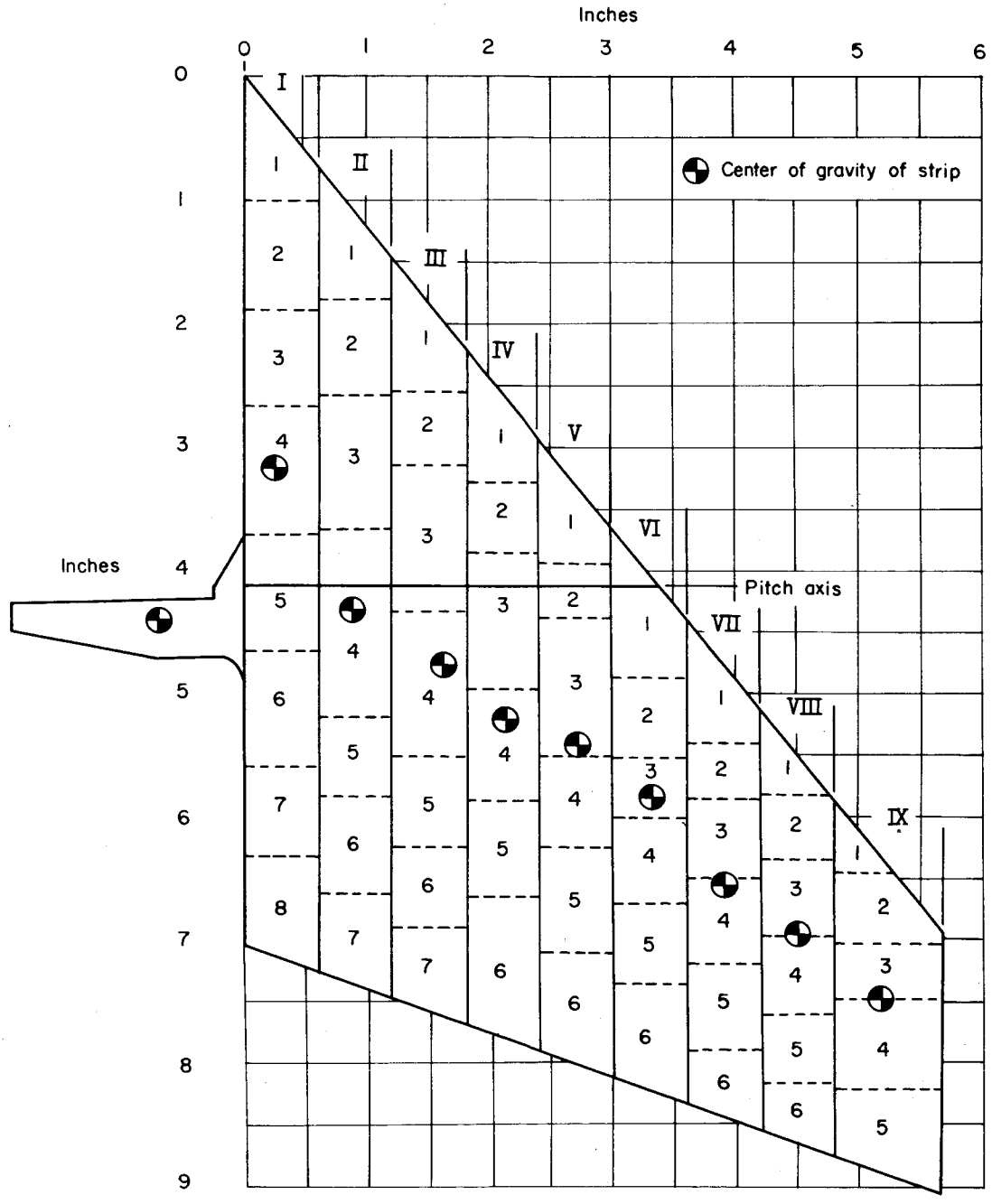

(a) Models HT-1H and HT-7C.

Figure 7.- Sketches of models of horizontal tail showing cuts made to determine mass parameters.

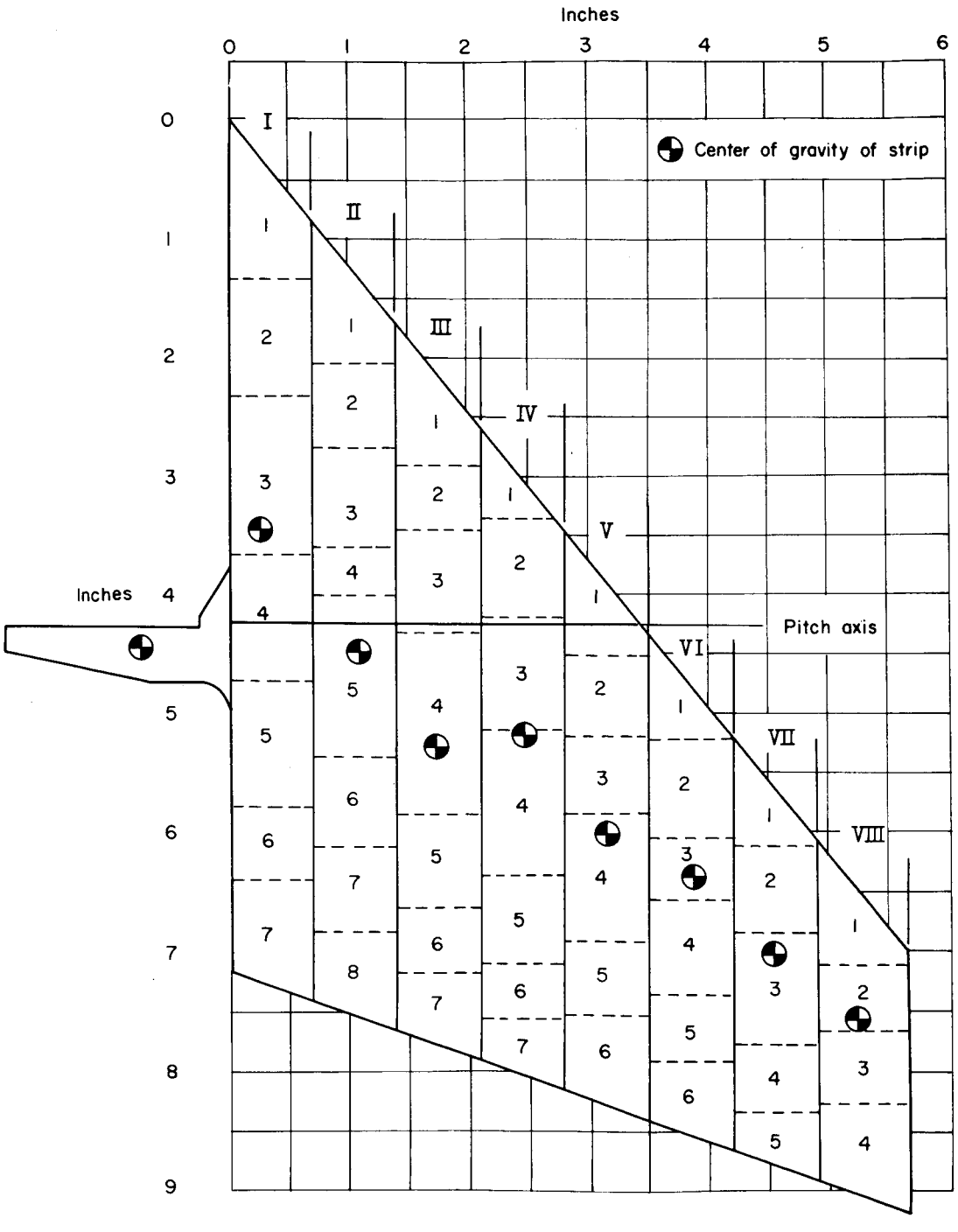

(b) Model HT-2H.

Figure 7.- Continued.

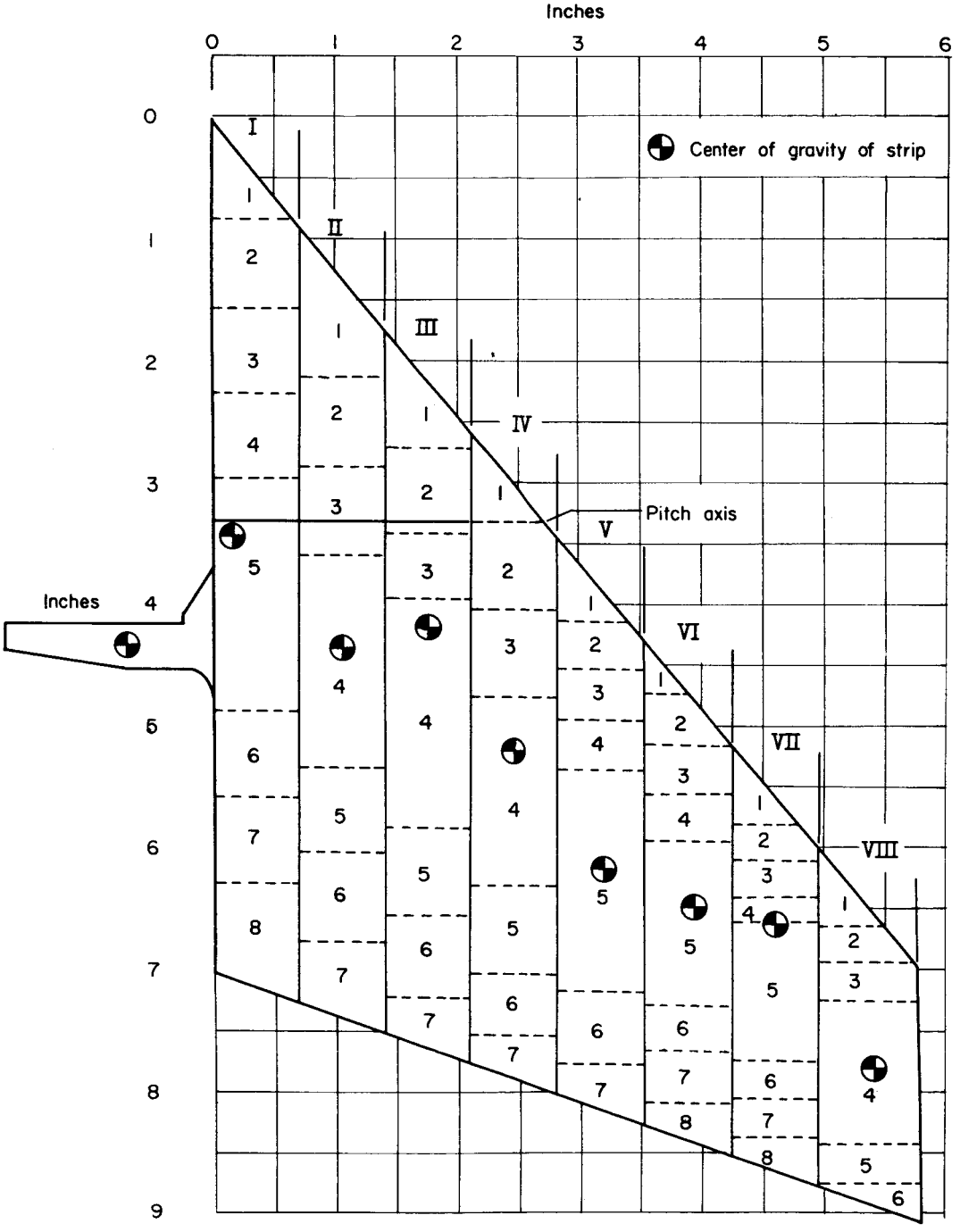

(c) Model HT-4H.

Figure 7.- Continued.

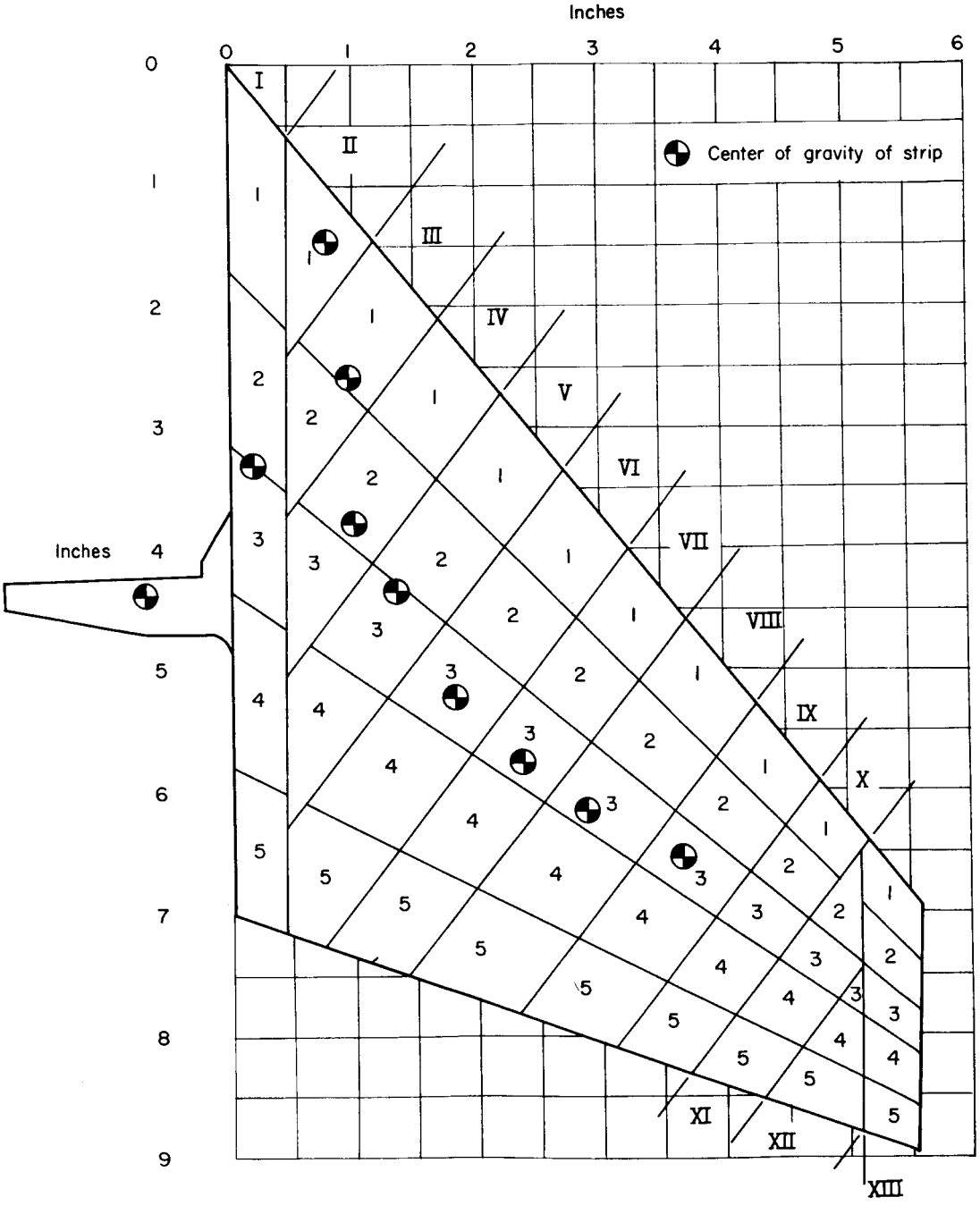

(d) Model HT-8H.

Figure 7.- Concluded.

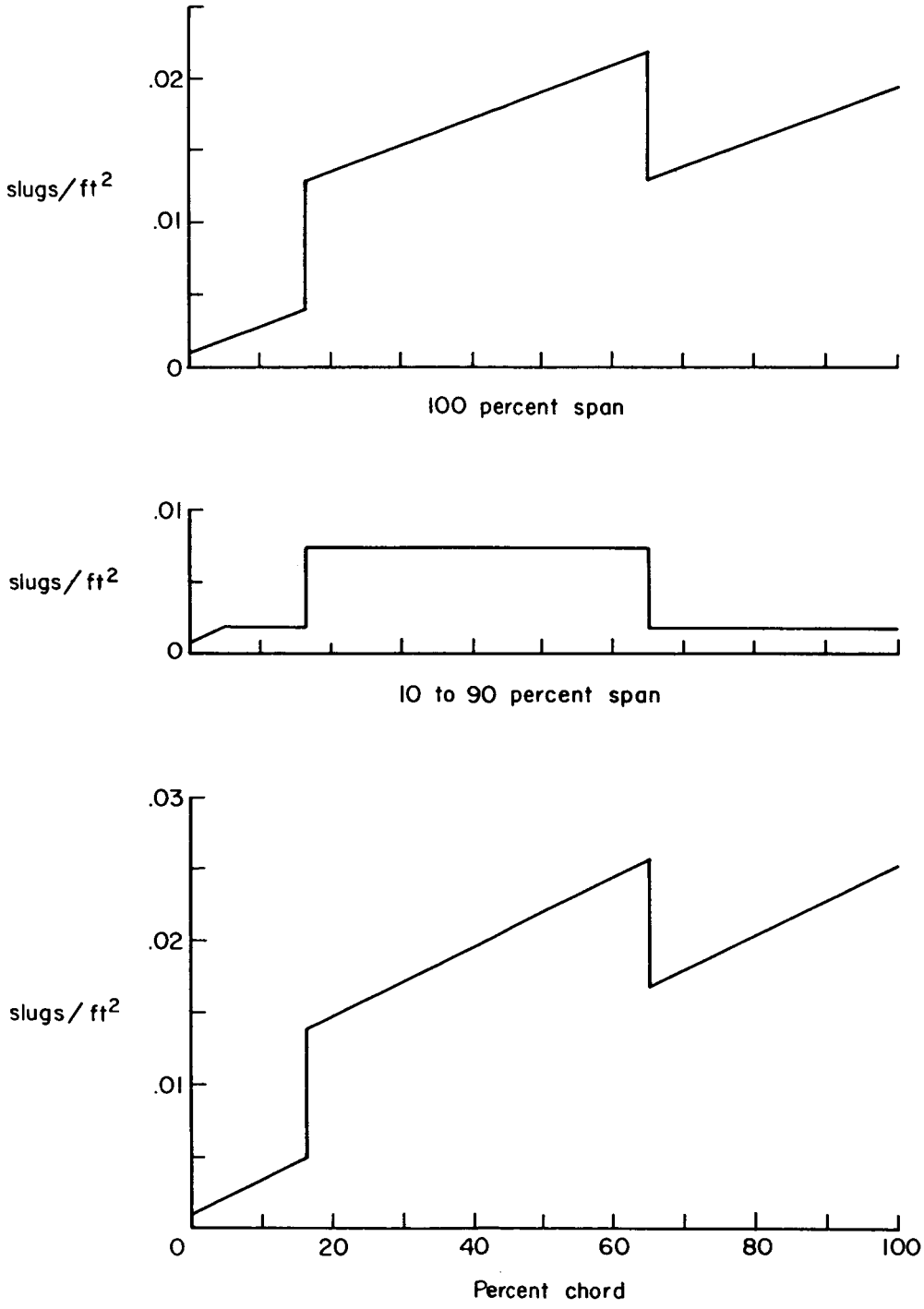

Figure 8.- Chordwise mass distribution curve for movable portion of model VT-2.

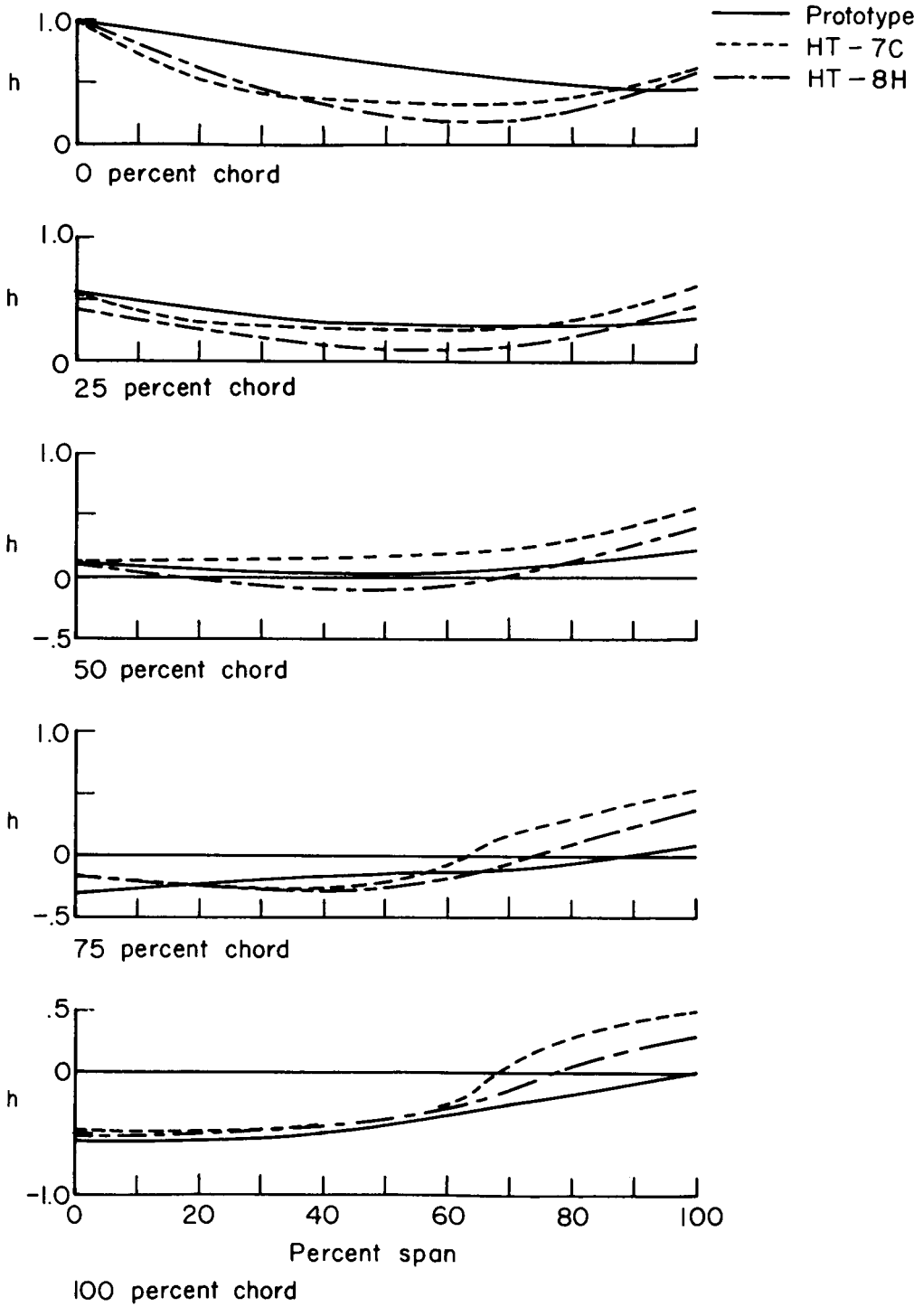

Figure 9.- Comparison of the shape of the second mode between model and prototype horizontal tails.

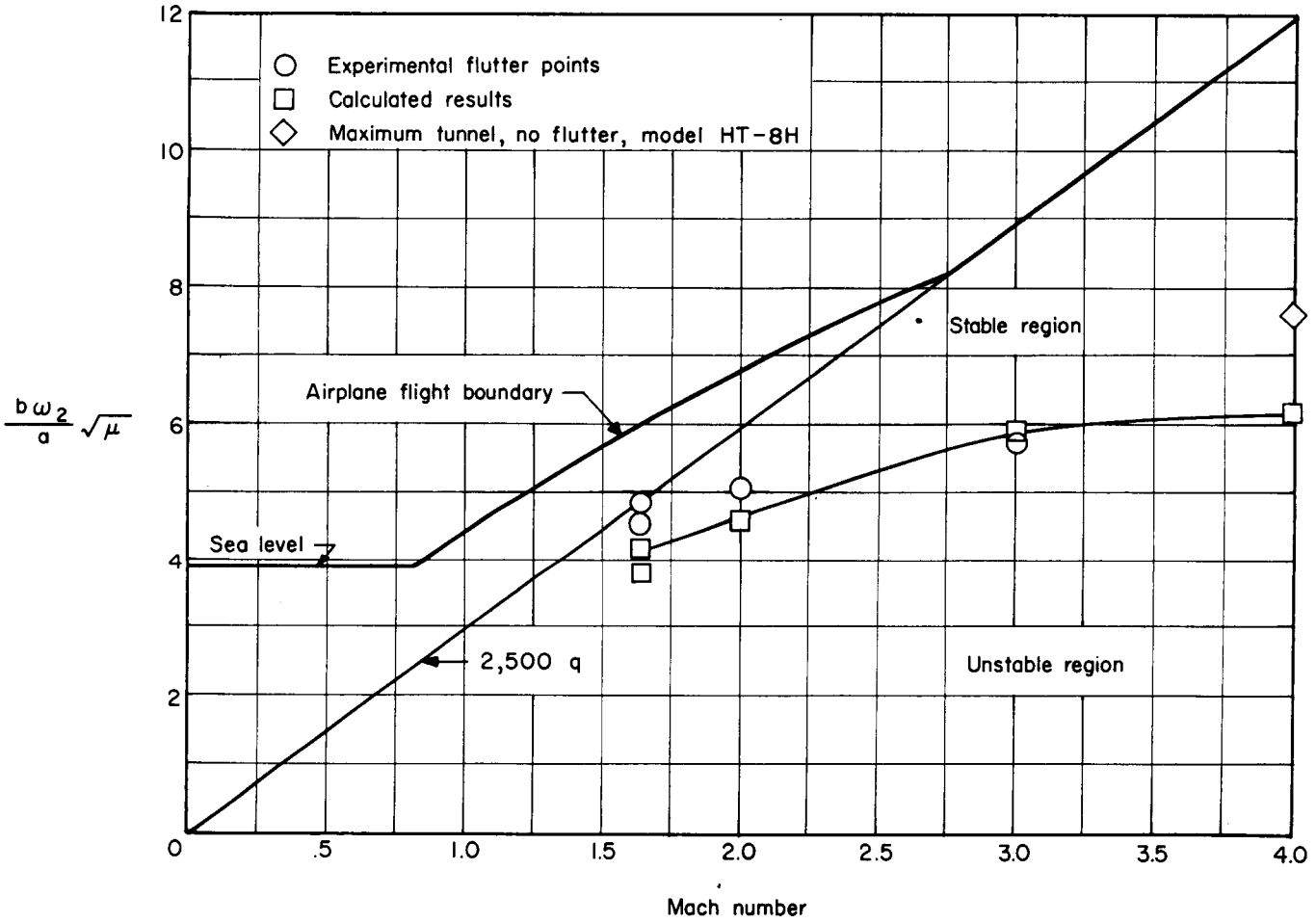

(a) Horizontal tails.

Figure 10.- Plot of stiffness-altitude parameter against Mach number showing experimental flutter points, calculated results, and 2,500q flight boundary.

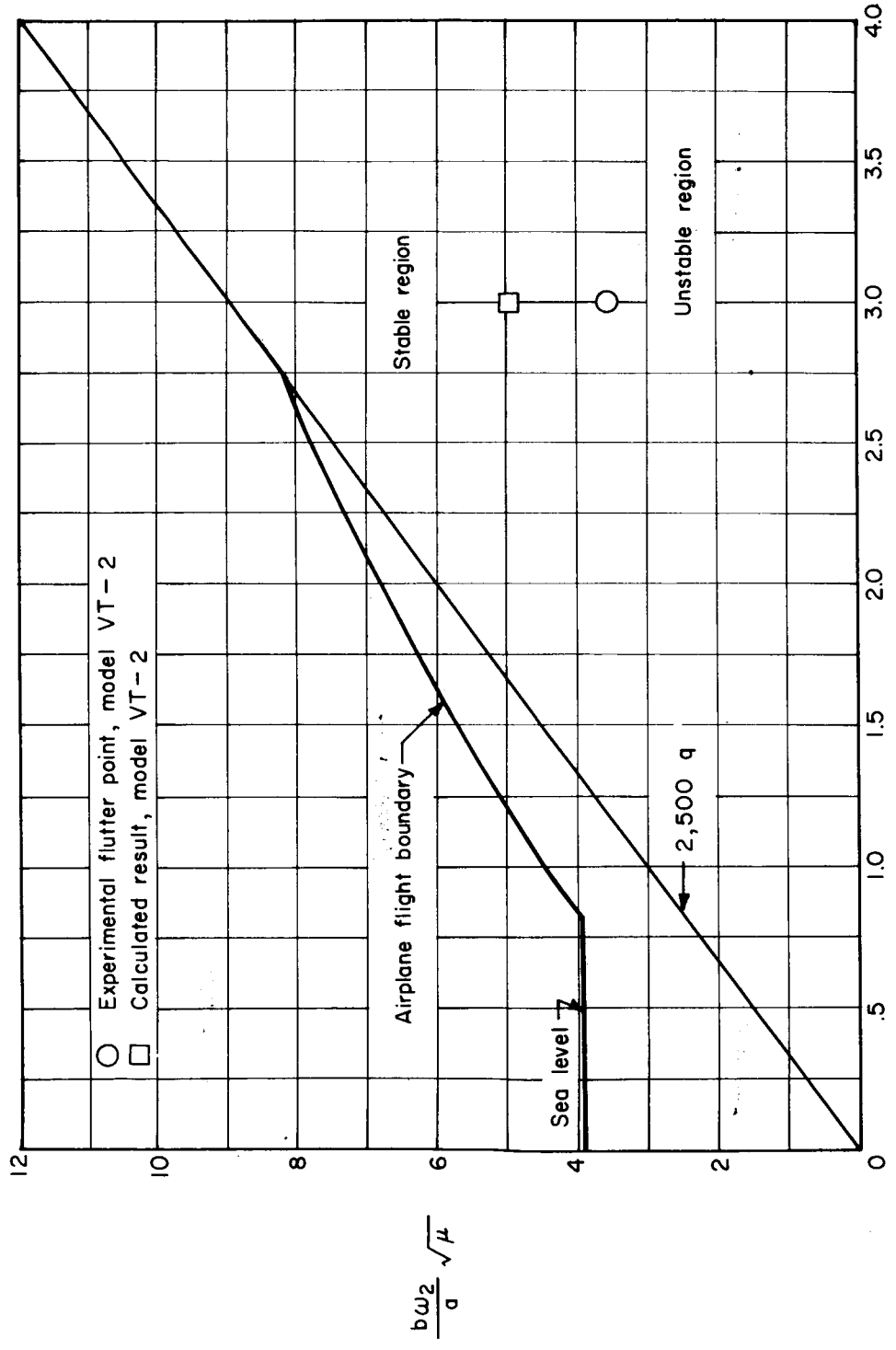

(b) Vertical tail.

Figure 10.- Concluded.